Activation and Kinetics of Circulating T Follicular Helper Cells, Specific Plasmablast Response, and Development of Neutralizing Antibodies following Yellow Fever Virus Vaccination

John Tyler Sandberg,* Sebastian Ols,† Marie Löfling,* Renata Varnaitė,* Gustaf Lindgren,‡ Ola Nilsson,§,¶,‖ Lars Rombo,#,‖ Markus Kalén,** Karin Loré,†,1 Kim Blom,*,1 and Hans-Gustaf Ljunggren*,1

A single dose of the replication-competent, live-attenuated yellow fever virus (YFV) 17D vaccine provides lifelong immunity against human YFV infection. The magnitude, kinetics, and specificity of B cell responses to YFV 17D are relatively less understood than T cell responses. In this clinical study, we focused on early immune events critical for the development of humoral immunity to YFV 17D vaccination in 24 study subjects. More specifically, we studied the dynamics of several immune cell populations over time and the development of neutralizing Abs. At 7 d following vaccination, YFV RNA in serum as well as several antiviral proteins were detected as a sign of YFV 17D replication. Activation of Th1-polarized circulating T follicular helper cells followed germinal center activity, the latter assessed by the surrogate marker CXCL13 in serum. This coincided with a plasmablast expansion peaking at day 14 before returning to baseline levels at day 28. FluoroSpot-based analysis confirmed that plasmablasts were specific to the YFV-E protein. The frequencies of plasmablasts correlated with the magnitude of neutralizing Ab titers measured at day 90, suggesting that this transient B cell subset could be used as an early marker of induction of protective immunity. Additionally, YFV-specific memory B cells were readily detectable at 28 and 90 d following vaccination, and all study subjects tested developed protective neutralizing Ab titers. Taken together, these studies provide insights into key immune events leading to human B cell immunity following vaccination with the YFV 17D vaccine. ***The Journal of Immunology*****, 2021, 207: 1033–1043.**

The recent outbreaks of yellow fever (YF) in South America and Sub-Saharan Africa demonstrate that YF remains a continuous serious global health problem despite the existence of an effective vaccine (1). According to the U.S. Center for Disease Control, there are an estimated 200,000 YF cases each year, causing around 30,000 deaths (2). There is no antiviral treatment for the infection, and vector control is difficult. Hence, the main method of controlling YF virus (YFV) infection is through vaccination of at-risk populations and travelers. The YFV 17D vaccine is noted as one of the best vaccines currently available because of its high efficacy and safety profile (3). A single dose can give lifelong immunity, and >95% of vaccinated individuals develop protective neutralizing Abs (3). The vaccine is comprised of an attenuated YFV (17D strain) that is replication competent and, upon administration, causes a mild, acute infection inducing a fine-tuned immune response leading to induction of protective immunity.

Numerous studies have investigated and corroborated the development of protective immunity following vaccination with YFV 17D by characterizing YFV-specific T cell and Ab responses. The YFV 17D vaccine has been shown to induce Ag-specific polyfunctional $CD8^+$ T cells that target numerous viral proteins following vaccination and exhibit strong functional memory response (4, 5). $CD4^+$ T cells have been described to expand early on after vaccination and precede the $CD8^+$ T cell response with a mixed Th1/Th2 phenotype (4, 6, 7). YFV 17D is also effective at inducing the generation of neutralizing Abs that have been detected in vaccinated individuals up to 60 years following vaccination (8, 9). Several serological studies using YFV 17D have elucidated that primary neutralizing activity of Abs is targeted toward the YFV-E protein, specifically targeting domains I and II (10, 11).

Interactions between B and T cells are required for the effective generation of protective neutralizing Abs and immunological memory. This interaction primarily occurs in the germinal centers of secondary lymphoid organs (12). During the germinal center reaction, a subset of cognate $CD4^+$ T cells, T follicular helper (Tfh) cells, help select high-affinity B cells undergoing class switching and affinity maturation. As a result, the selected high-affinity B cells differentiate into plasmablasts, plasma cells, or memory B cells (13).

*Center for Infectious Medicine, Department of Medicine Huddinge, Karolinska Institutet, Stockholm, Sweden; †Division of Immunology and Allergy, Department of Medicine Solna, Karolinska Institutet, Stockholm, Sweden; ‡Cell Therapy and Allogenic Stem Cell Transplantation, Karolinska University Hospital, Stockholm, Sweden; §Division of Pediatric Endocrinology, Karolinska University Hospital, Stockholm, Sweden; ¶Center for Molecular Medicine, Department of Women's and Children's Health, Karolinska Institutet, Stockholm, Sweden; ‖School of Medical Sciences, Örebro University and University Hospital, Örebro, Sweden; #Center for Clinical Research, Eskilstuna, Sörmland, Sweden; and **Department of Infection Medicine, Mälarsjukhuset, Eskilstuna, Sweden

[1]K.L., K.B., and H.-G.L. are cosenior authors.

ORCIDs: 0000-0001-6747-6933 (J.T.S.); 0000-0001-9784-7176 (S.O.); 0000-0001-9391-9291 (R.V.); 0000-0002-9986-8138 (O.N.); 0000-0002-5859-3158 (L.R.); 0000-0003-0908-7387 (H.-G.L.).

Received for publication December 7, 2020. Accepted for publication June 7, 2021.

This work was supported by the Vetenskapsrådet (2015-02499 to H.-G.L.), the Swedish Foundation for Strategic Research (SB12-0003 to H.-G.L.), the Centrum för Innovativ Medicin, Region Stockholm (2020-2022 to K.B.), and the KID Ph.D. student funding program from Karolinska Institutet (2-1930-2016 and 2016-00132 to J.T.S. and S.O.).

Address correspondence and reprint requests to Kim Blom, Center for Infectious Medicine, ANA Futura, Department of Medicine Huddinge, Karolinska Institutet, Alfred Nobels Allé 8, 141 52 Stockholm, Sweden. E-mail address: kim.blom@ki.se

The online version of this article contains supplemental material.

Abbreviations used in this article: cTfh, circulating Tfh; Tfh, T follicular helper; YF, yellow fever; YFV, YF virus.

Studying these interactions in vivo in humans is difficult. Recently, however, circulating $CD4^+$ T cells expressing CXCR5, named circulating Tfh (cTfh) cells, have been suggested as a peripheral counterpart of Tfh cells with similar function (14). Increases in activated cTfh cell frequencies in peripheral blood have been shown to positively correlate with high-avidity Ab responses after influenza vaccination in humans and are therefore a target of interest to further understand and improve vaccination strategies (15). Interestingly, a recent study also showed that YFV-specific, Th1-polarized cTfh cells increased in circulation following vaccination with YFV 17D and correlated with the strength of neutralizing Ab response (16).

The magnitude, kinetics, and specificity of the B cell response to YFV 17D have not been as extensively studied as T cell responses. Recent studies on early B cell responses to vaccination with YFV 17D indicate that there is an expansion of plasmablasts in peripheral blood 7–14 days postvaccination (16–19). A proportion of the plasmablast population were shown to secrete YFV-specific Abs, as assessed by ELISA (18). YFV-specific memory B cells have also been shown to appear in peripheral blood as early as 14 d, peaking at three to six months following vaccination with YFV 17D (18).

In this study, we set out to investigate the kinetics of the humoral immune response to YFV 17D by combining assessments of the magnitude and specificity of the plasmablast and Ab responses as well as the accompanying cTfh response. Activated Th1-polarized cTfh cell frequencies increased in circulation during the first weeks following vaccination in addition to increased germinal center activity. YFV-E–specific plasmablast responses coincided with cTfh cell activation and peaked two weeks following vaccination, as assessed using a FluoroSpot assay. Both YFV-E–specific memory B cells and neutralizing Abs were generated 28 and 90 d after vaccination. Additionally, the IgG^+ plasmablast frequency at day 14 correlated with protective neutralizing Ab titers detected at day 90. The present study adds, to our knowledge, novel insights into processes associated with the development of protective B cell immunity to YFV 17D vaccination.

Materials and Methods

Ethics statement and study subjects

A total of 24 healthy study subjects between the ages of 18 and 50 y (median age), who were not previously vaccinated against or infected with YFV, received a single dose of the YFV 17D vaccine, Stamaril (Sanofi Pasteur). All the study subjects gave written, informed consent to participate. The Regional Ethical Review Board in Stockholm, Sweden, approved the study.

Sample collection

Serum and whole blood were collected before vaccination (day 0, $n = 24$) and at days 7 ($n = 15$), 14 ($n = 24$), 28 ($n = 18$), and 90 ($n = 12$) (Fig. 1A). Blood samples were collected in EDTA vacuum tubes and in serum clot activator tubes (Greiner Bio-One Vacuette). PBMCs were isolated by Lymphoprep gradient centrifugation and cryopreserved in FCS with 10% DMSO at −180°C or used fresh for experiments. Serum was isolated after separation from clotted blood through centrifugation and frozen at −80°C for future analyses.

Determination of YFV RNA levels in serum

YFV-specific real-time PCR was used to determine the viral load in serum of vaccinees. RNA was isolated from 150 μl of serum using a NucleoSpin RNA Virus Kit (Machery-Nagel). One step real-time PCR was performed using TaqMan Fast Virus 1-Step Master Mix (Applied Biosystems), an FAM-TAMRA–labeled probe and primers (Fisher Biotechnology) according to the manufacturer's instructions. The primers and probe were all specific for the highly conserved NS5 gene of YFV (20) and were used at a final concentration of 800 and 125 nM for the primers and probe, respectively. Amplifications were performed in 25-μl reactions using a QuantStudio 5 Real-Time PCR machine (Applied Biosystems) under the following thermal cycling conditions: 5 min at 50°C, 20 s at 95°C, 45 cycles of 15 s at 95°C, followed by 1 min at 60°C. RNA from the YFV 17D was calibrated to a standard curve commercially available in the Techne quantitative PCR test for YFV (Techne) and used for quantification. Limit of detection was 20 copies/ml.

Assessment of serum protein levels

A total of 92 protein biomarkers were measured in serum of 10 randomly selected study subjects from days 0, 7, and 14 by proximity extension assay using the Immune Response panel at Olink Bioscience, Uppsala, Sweden, as previously described (21). The protein biomarkers were detected using Ab pairs labeled with specific oligonucleotides that, when in close proximity, hybridize. Their DNA barcodes were subsequently quantified by real-time PCR. Protein levels are reported in arbitrary units, normalized protein expression. This arbitrary unit can be used for relative protein quantification as well as for comparing fold changes between time points. Of the 92 proteins measured, 87 were detectable within quality control range.

YFV-E protein conjugation

Two preparations of fluorophore-conjugated YFV-E protein (Abbexa) were prepared using a Lightning-Link tandem conjugation kit for FluoroSpot assay, according to the manufacturer's instructions (Expedeon). Briefly YFV-E protein concentration was adjusted to 1 mg/ml using PBS and 1 μl of Lightning-Link–modifier reagent was added for each 10 μl of protein solution to be conjugated. This solution was directly added onto the lyophilized fluorophore and incubated at room temperature in the dark for 15 min. Following incubation, 1 μl Lightning-Link quencher for each 10 μl protein solution was added for 30 min. Aliquots of conjugated protein were stored at −20°C before use.

Flow cytometry

Freshly isolated PBMCs were used for phenotypical analysis using the following Abs: LIVE/DEAD cell marker Near-IR (Life Sciences), anti-CD19 (clone SIJ25C1) BUV 395, anti-CD4 (clone SK3) BUV 737, anti-CD16 (clone 3GB) Pacific Blue, anti-CD14 (clone MφP9) AmCyan, anti-Ki67 (clone B56) Alexa Fluor 700 (BD Biosciences), anti-CD20 (clone 2H7) FITC, anti-CD123 (clone 6H6) AmCyan, anti-CD27 (clone O323) BV650, anti-CD38 (clone HIT2) BV785, anti-IgD (clone IA6-2) PE-Cy7, anti-IgG (clone HP6017) PE (BioLegend), anti-CD56 (clone N901) Electron Coupled Dye, anti-CD3 (clone UCHt1) PE-Cy5 (Beckman Coulter), anti-CD8 (clone 3B5) Qdot 605 (Invitrogen), and anti-IgA (clone IS11-8E10) APC (Miltenyi Biotec). For staining, cells were incubated with optimized concentrations of surface marker Abs diluted in FACS buffer (PBS, 2% FCS, and 2 mM EDTA) in the dark for 30 min at 4°C. Cells were then washed twice with FACS buffer and then fixed and permeabilized with Foxp3/transcription factor staining suffer (Invitrogen) for 30 min at 4°C in the dark. For intracellular staining, cells were incubated with optimized concentrations of Abs against Ki67 and IgG in the dark for 30 min at 4°C. Samples were acquired with a BD LSRFortessa (BD Biosciences), followed by analysis with FlowJo software version 10 (FlowJo). B cell activation and plasmablasts were defined from an extended lymphocyte gate as live $CD14^-CD123^-CD3^-CD19^+CD38^+Ki67^+$ and live $CD14^-CD123^-CD3^-CD19^+CD20^{-/low}CD27^{high}CD38^{high}$ cells, respectively, and the percentage of plasmablasts among total $CD19^+$ B cells was determined. Expression of IgG, IgA, and Ki67 was further assessed on plasmablasts. The remaining cell subsets were defined from a normal lymphocyte gate. T cell activation was defined as live $CD14^-CD123^-CD19^-CD3^+CD8^+/CD4^+Ki67^+CD38^+$ cells. NK cells were identified as live $CD14^-CD123^-CD19^-CD3^-CD16^+$ cells with varying expression of CD56 defined as $CD56^{bright}$ or $CD56^{dim}$ cells and their activation determined by Ki67 and CD38 coexpression. (Supplemental Fig. 1A).

Cryopreserved PBMCs were thawed and stained for further phenotypical analysis using the following Abs: anti-CD19 (clone SJ25C1) BUV395, anti-PD1 (clone EH12.1) BUV737, anti-Ki67 (clone B56) Alexa Fluor 700, anti-CD14 (clone MφP9) V500 (BD Biosciences), anti-CD20 (clone 2H7) FITC, anti-ICOS (clone C398.4A) APC/Cy7, anti-CCR7 (clone G053H7) BV421, anti-CD27 (clone O323) BV650, anti-CXCR5 (clone J252D4) BV711, anti-CXCR3 (clone G025H7) BV785, anti-IgG (clone M1310G05) PE, anti-IgD (clone IA6-2) PE/Cy7 (BioLegend), anti-IgA (clone IS11-8E10) APC (Miltenyi Biotec), Aqua LIVE/DEAD cell marker, anti-CD4 (clone S3.5) Qdot 605 (Invitrogen), and anti-CD3 (clone UCHT1) PC5 (Beckman Coulter). For staining, cells were incubated with optimized concentrations of surface marker Abs diluted in FACS buffer (PBS, 2% FCS, and 2 mM EDTA) in the dark for 15 min at 37°C. Cells were then washed twice with FACS buffer and then fixed and permeabilized with Foxp3/transcription factor staining suffer (Invitrogen) for 30 min at 4°C in the dark. For intracellular staining, cells were incubated with an optimized concentration of anti-Ki67 Ab in the dark for 30 min at 4°C. Samples were acquired with a BD LSRFortessa (BD Biosciences), followed by analysis with FlowJo software version 10 (FlowJo). B cells were defined as live $CD3^-CD19^+CD20^+$ and memory B cells as $CD27^+IgD^-$, unswitched memory B cells as $CD27^+IgD^+$, naive B cells as $CD27^-IgD^+$, and double-negative B cells as $CD27^-IgD^-$. Memory B cells were further divided into

IgG^+ or IgA^+ subsets. Homing status of all B cell subsets were determined using CXCR5-, CXCR3-, and CCR7-expression analysis. cTfh cells were defined as live $CD3^+CD4^+CXCR5^+$ cells and further divided into $CXCR3^{+/-}$ subsets. Activated phenotypes of cTfh cells and subsets were assessed by single or coexpression of CCR7, PD1, ICOS, and Ki67 (Supplemental Fig. 1B).

FluoroSpot assay

Total IgG^+ and IgA^+ plasmablasts as well as YFV-E–specific IgG^+ plasmablasts and memory B cells were measured using a multicolor FluoroSpot kit (Mabtech) according to the manufacturer's instructions with some in-house modifications. Briefly, ethanol-activated low autofluorescent polyvinylidene difluoride membrane plates were coated with 100 µl capture anti-IgG and anti-IgA Abs at 15µg/ml in PBS overnight. YFV-E–specific wells were coated with only capture anti-IgG. Cryopreserved PBMCs were thawed, counted, and allowed to rest 1 h in warm R10 media (RPMI 1640 supplemented with 10% heat-inactivated FCS, 1% penicillin/streptomycin, and 1% L-glutamine). For memory B cell FluoroSpot, rested PBMCs were stimulated with 1 µg/ml R848 and 10 ng/ml recombinant human IL-2 for 3 d before being counted and used in the assay. The coated plates were washed and blocked with R10 media for 30 min before several dilutions of rested or stimulated PBMCs were added to each well. Plates were incubated at 37°C 5% CO_2 for up to 24 h, and total wells were developed with 100 µl/well anti-human IgG-550 and anti-human IgA-490 at 1:500 in PBS containing 0.5% BSA, whereas YFV-E–specific wells were developed with anti-human IgG-550 at 1:500 and YFV-E Cy5 (Abbexa and Expedeon) at 0.5 µg/ml in PBS containing 0.5% BSA. Spots were detected with a Mabtech IRIS and counted with Apex software (Mabtech).

CXCL13 ELISA

Undiluted serum was thawed at room temperature and analyzed using a Quantikine Human CXCL13/BLC/BCA-1 ELISA (R&D Systems) according to the manufacturer's instructions. Briefly, 100 µl of Assay Diluent RD1S was added to each well of the anti-human CXCL13–coated, 96-well microplate. A total of 50 µl of standards, controls, or undiluted serum samples were added and incubated for 2 h at room temperature. Wells were washed four times using provided wash buffer in a squirt bottle. A total of 200 µl of anti-human CXCL13 conjugate was then added to each well and incubated for 2 h at room temperature. Wells were washed four times, followed by addition of 200 µl of substrate solution incubated for 30 min at room temperature in the dark. Following incubation, 50 µl of stop solution was added to each well, and the OD of each well was measured immediately using a Tecan microplate reader set to 450 nm and analyzed using Magellan software (Tecan). Results were calculated using ElisaAnalysis.com (Leading Technology Group) to generate a standard curve to calculate CXCL13 concentrations. The limit of detection of the assay ranges between 7.8 and 500 pg/ml.

Virus neutralization assay

Virus neutralization was measured by rapid fluorescent focus inhibition test at the Public Health Agency of Sweden as previously described with modifications for YFV (22). Briefly, serum from days 0, 28, and/or 90 were heat inactivated and tested at dilutions of 1:5 and 1:20 with ∼50 50% focus-forming doses of YFV *Asibi* strain in 96-well plates. Following incubation of serum and virus, BHK-21 cells were added to each well, and the plates were incubated for 24 h and later fixed with 80% acetone. After fixation, virus foci were detected by fluorescent staining. In each well, 20 microscopic fields were examined for fluorescent foci, and those with one or more foci were recorded. Titers are defined as ED_{90} and reciprocal titers of ED_{90} ≥5 were deemed positive.

Statistical analyses

Statistical analyses were performed using GraphPad Prism version 9 (GraphPad Software). Datasets were analyzed using nonparametric Wilcoxon matched-pairs signed-rank test or Friedman or Spearman rank tests. Dunn multiple comparisons test was used to correct for multiple comparisons when applicable. Any p values <0.05 were considered to be statistically significant. Serum protein normalized protein expression analyses' p values were adjusted by false discovery rate using the Benjamini–Hochberg method with Q value set at 5%.

Results

Viral RNA and immune response–related protein levels in serum following YFV 17D vaccination

The vaccination and sampling strategy is depicted (Fig. 1A). To confirm YFV 17D replication following vaccination in the study subjects, we first measured viral load in serum. YFV RNA was detected in 9 out of 14 tested study subjects on day 7 (Fig. 1B). By day 14, no remaining YFV RNA was detected in serum in any of the study subjects, as we and others have previously demonstrated (20, 23).

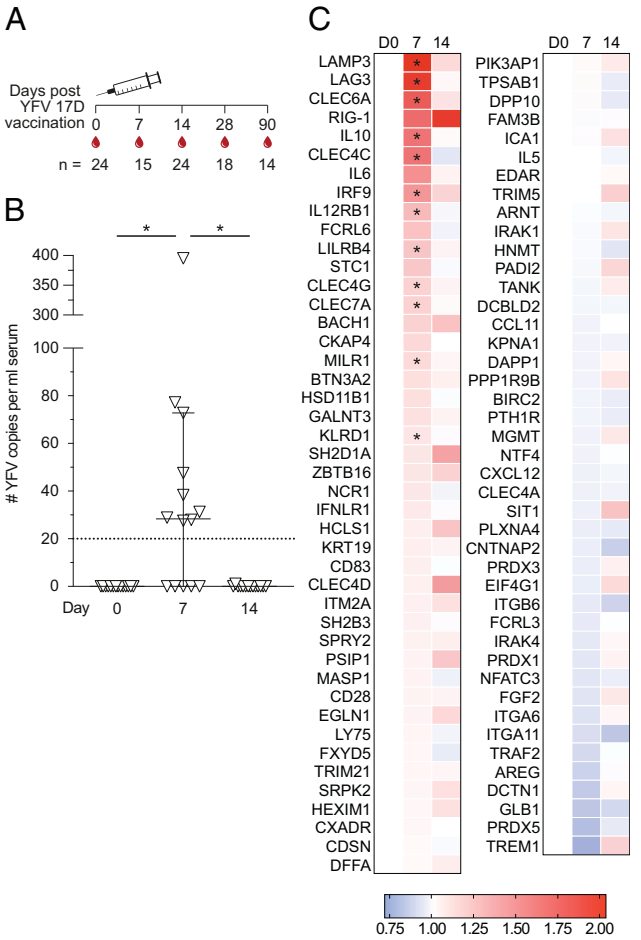

FIGURE 1. Vaccination strategy and detection of viral RNA and immune response–related proteins in serum following YFV 17D vaccination. (**A**) Vaccination and sampling schedule for all study subjects (n = 24). (**B**) YFV NS5 copies in serum as detected by RT-PCR. Dotted line at y = 20 denotes limit of detection. Plots represent median with 95% confidence interval (CI) (n = 14). (**C**) Fold change day 7 and day 14, in comparison with day 0, of 87 immune response–related proteins (n = 10). Statistical analysis was performed using nonparametric Friedman test and corrected for multiple comparisons with Dunn multiple comparison test. The protein comparison p values were adjusted by false discovery rate using the Benjamini–Hochberg method with Q value set at 5%.*$p < 0.05$.

A screen of 92 immune response–related proteins in serum coincided with replication of YFV 17D evidenced by a significant increase of antiviral proteins at day 7. These included retinoic acid–inducible gene 1 (RIG-I), IFN regulatory factor 9 (IRF9), and cytoskeleton-associated protein 4 (CKAP4) (Fig. 1C). Following testing for false discovery rates in changes over time, 12 proteins were identified as significantly increased following vaccination and further analyzed using the ABsolute Immune Signal deconvolution Shiny App tool (24), revealing cell types in which these proteins predominantly are expressed (Supplemental Fig. 2). This analysis revealed a large portion of proteins expressed by several innate immune cells, T cells, and B cells. Expression levels of a number of pro- and anti-inflammatory as well as antiviral proteins were also identified as significantly increased at day 7 following vaccination (Supplemental Fig. 2).

NK, T, and B cell activation following YFV 17D vaccination

Surface expression of CD38 and intracellular expression of Ki67 on freshly isolated PBMCs were initially used to determine the

magnitude and kinetics of activation and proliferation of NK, T, and B cells in response to YFV 17D vaccination over time (Fig. 2A, 2D, 2G). Activation in both $CD56^{bright}$ and $CD56^{dim}$ NK cells was shown to increase following vaccination, peaking at day 7 in $CD56^{bright}$ cells and at day 14 in $CD56^{dim}$ NK cells before returning to baseline levels (Fig. 2B, 2C). Activation of $CD4^+$ and $CD8^+$ T cells similarly increased following vaccination, peaking at day 14 (Fig. 2E, 2F). $CD4^+$ T cell activation preceded that of $CD8^+$ T cells with detectable responses observed already at day 7 (Fig. 2F). T cell activation levels returned to baseline levels at day 28 (Fig. 2E, 2F). B cells, defined as live $CD3^-CD19^+$ cells, also revealed significant activation following vaccination. A strong increase in B cell activation and proliferation in circulation was observed at day 7 following vaccination. This continued and peaked at day 14, after which activated cells returned to baseline levels (Fig. 2H). Altogether, the data show that the increase in YFV replication coincided with NK cell, CD4 T cell, and B cell activation and expansion and preceded the CD8 T cell response and peak B cell response by 1 wk, in line with previous work (4, 23). With these early observations in hand, we went on to characterize the events leading up to the generation of neutralizing Abs and YFV-specific B cell responses.

cTfh cell frequencies following YFV 17D vaccination

As noted above, activated $CD4^+$ T cell frequencies were observed to increase already in the first week following vaccination with YFV 17D. Among $CD4^+$ T cells, cTfh cells are defined as $CD4^+CXCR5^+$ T cells, and their subsets can further be defined based on their CXCR3 expression (Fig. 3A). Frequencies of total cTfh cells as well as Th2/17-polarized $CXCR3^-$ cTfh cells generally did not change over time; however, a nonsignificant decrease in frequency of Th1-polarized $CXCR3^+$ cells at day 7 was observed that then returned to baseline levels by days 14 and 28 following

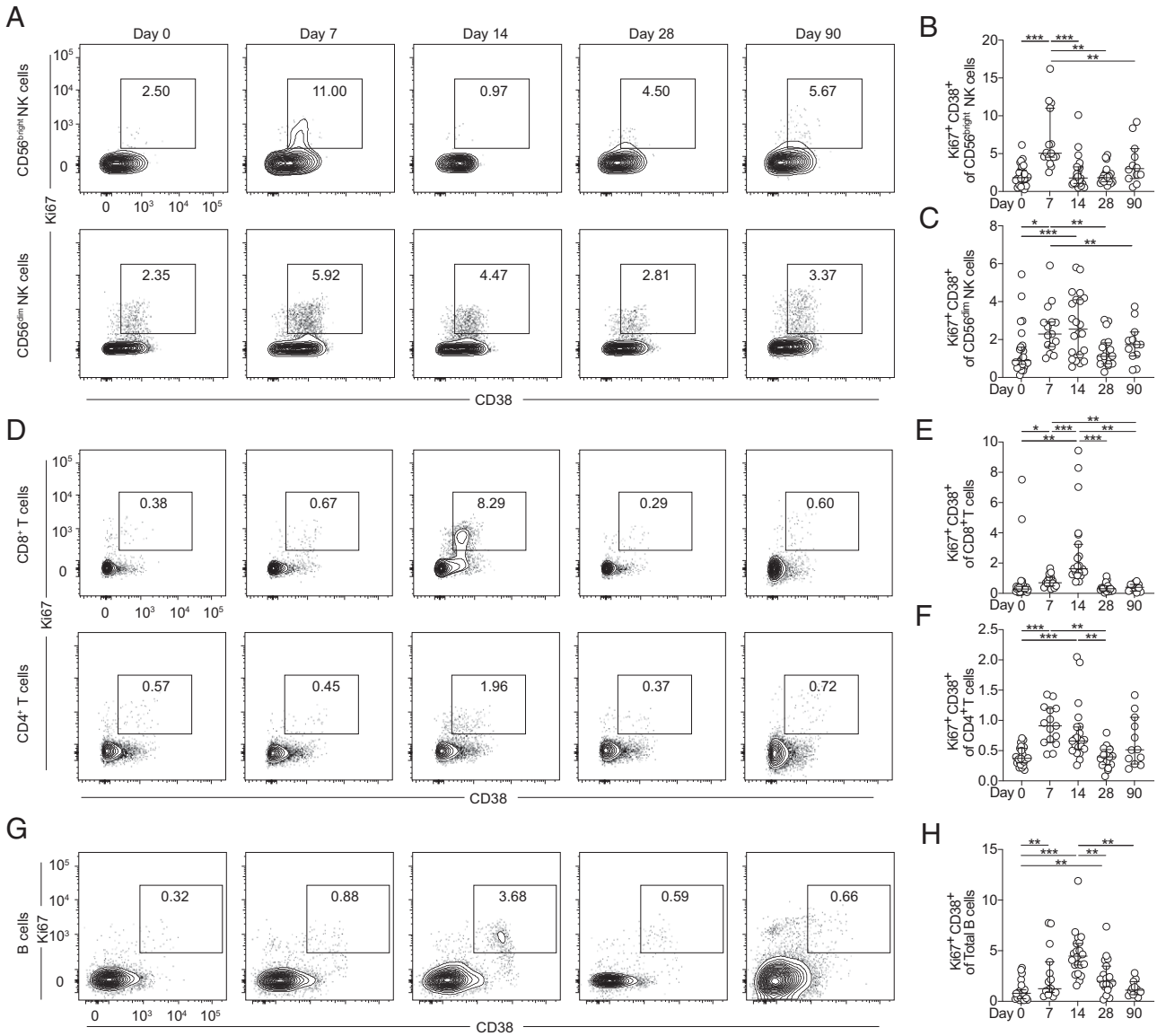

FIGURE 2. Magnitude and kinetics of NK, T, and B cell activation following YFV 17D vaccination. (**A**) CD38 and Ki67 coexpression on freshly isolated $CD56^{bright}$ and $CD56^{dim}$ cells over time in one representative study subject. Plot of CD38 and Ki67 coexpression on (**B**) $CD56^{bright}$ and (**C**) $CD56^{dim}$ cells at days 0, 7, 14, 28, and 90 following vaccination. (**D**) CD38 and Ki67 coexpression on freshly isolated $CD8^+$ and $CD4^+$ T cells over time in one representative study subject. Plots of CD38 and Ki67 coexpression on (**E**) $CD8^+$ T cells and (**F**) $CD4^+$ T cells at days 0, 7, 14, 28, and 90 following vaccination. (**G**) CD38 and Ki67 coexpression on freshly isolated $CD19^+$ B cells over time in one representative study subject. (**H**) Plots of CD38 and Ki67 coexpression on B cells at days 0, 7, 14, 28, and 90 after vaccination. All plots represent median with 95% confidence interval (CI). For all plots: day 0, $n = 24$; day 7, $n = 15$; day 14, $n = 22$; day 28, $n = 18$; and day 90, $n = 12$. Statistical analysis was performed using nonparametric Wilcoxon matched-pairs signed-rank test. $*p < 0.05$, $**p < 0.01$, $***p < 0.001$.

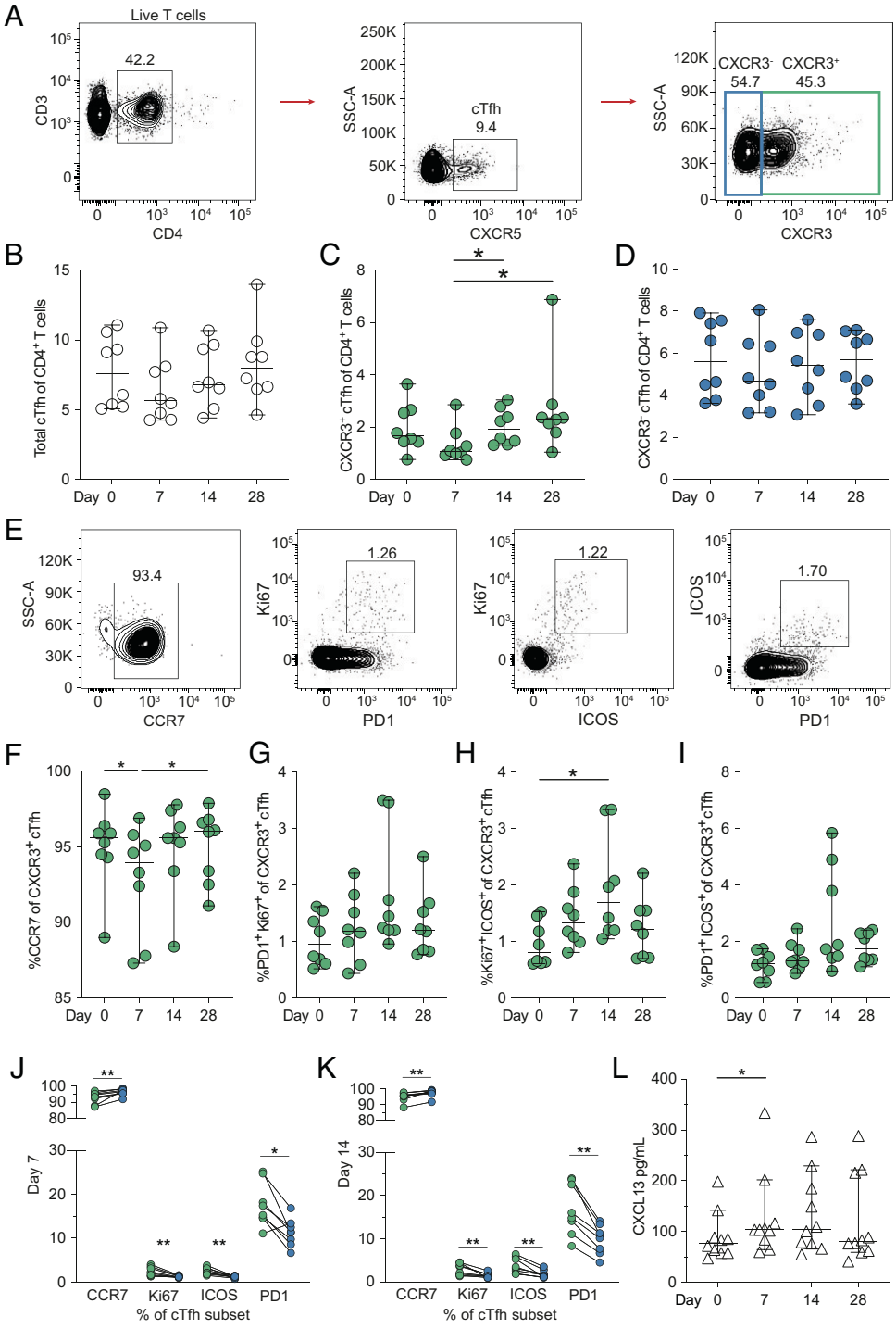

FIGURE 3. cTfh cells and germinal center activity following YFV 17D vaccination. (**A**) Gating strategy of cTfh cells defined as $CXCR5^+$ $CD4^+$ T cells with Th1-polarized $CXCR3^+$ and Th2/17-polarized $CXCR3^-$ subsets. (**B**) Total cTfh, (**C**) Th1-polarized $CXCR3^+$ cTfh, and (**D**) $CXCR3^-$ cTfh cell frequencies of $CD4^+$ T cells over time following vaccination. (**E**) Representative gating of frequencies of Th1-polarized $CXCR3^+$ cTfh cells expressing CCR7, Ki67, ICOS, and PD1. (**F**) Expression of CCR7 and activation of Th1-polarized $CXCR3^+$ cTfh cells over time as assessed by dual expression of (**G**) PD1 and Ki67, (**H**) ICOS and Ki67, and (**I**) PD1 and ICOS. Comparison of expression of CCR7, Ki67, ICOS, and PD1 between Th1-polarized $CXCR3^+$ (green) and Th2/17-polarized $CXCR3^-$ (blue) cTfh cells on (**J**) day 7 and (**K**) day 14 following vaccination. (**L**) Change in germinal center activity over time as defined by serum CXCL13 concentrations determined by ELISA (n = 10). All graphs plotted as median with 95% confidence interval (CI) (n = 8 unless otherwise stated). Statistical analysis was performed using nonparametric Friedman test and corrected for multiple comparisons with Dunn multiple comparison test (B–D, F–I, and L) or nonparametric Wilcoxon matched-pairs signed-rank test. $^*p < 0.05$, $^{**}p < 0.01$.

YFV 17D vaccination (Fig. 3B–D). Expression of CCR7 and coexpression of Ki67, ICOS, and PD1 were used to assess Th1-polarized $CXCR3^+$ cTfh cell activation (Fig. 3E). Cells expressing CCR7 transiently decreased at day 7 following vaccination (Fig. 3F). Th1-polarized $CXCR3^+$ cTfh cells coexpressing PD1 and Ki67 (Fig. 3G), Ki67 and ICOS (Fig. 3H), and PD1 and ICOS (Fig. 3I) were also assessed over time following YFV 17D vaccination. Only cells coexpressing Ki67 and ICOS were observed to significantly increase between day 0 and 14, however. Additionally, we also examined differences in activation of Th1-polarized $CXCR3^+$ and Th2/17-polarized $CXCR3^-$ cTfh cells at days 7 (Fig. 3J) and 14 (Fig. 3K) following vaccination. The Th1-polarized $CXCR3^+$ cTfh cell population was shown to increase in expression of Ki67, ICOS, and PD1, whereas a decrease in CCR7 expression was observed at both time points. This activation suggests the antiviral Th1-polarized population to be the primary cTfh response to YFV 17D vaccination. As cTfh cell activation serves as a marker of activity in secondary lymphoid organs, we set out to confirm germinal center activation by measuring soluble CXCL13 levels in serum.

CXCL13 serum levels following YFV 17D vaccination

CXCL13 levels in serum, functioning as a surrogate marker of germinal center activation (25), were measured before and at days 7, 14, and 28 following vaccination. Levels of CXCL13 increased slightly at day 7 before returning to baseline levels by day 28 (Fig. 3L). This increase in serum CXCL13 levels and Th1-polarized $CXCR3^+$ cTfh activation indicates germinal center activation in secondary lymphoid organs following vaccination with YFV 17D.

With germinal center activity assessed, we then set out to measure the magnitude, kinetics, and specificity of B cell responses.

Plasmablast frequencies following YFV 17D vaccination

As noted above, the increase in activation of B cells was observed in the first weeks following YFV 17D vaccination. Upon further investigation, plasmablast expansion was deemed responsible for this increase. Plasmablasts were analyzed from freshly isolated PBMCs (Fig. 4A). Baseline levels of plasmablasts averaged <1% of the total B cell population (Fig. 4B). Plasmablast frequencies were expanded at day 7 following YFV 17D vaccination and peaked at day 14 before returning to baseline levels by day 28 (Fig. 4B). Further analysis of IgA^+, IgG^+, and IgG^-IgA^- plasmablast subsets revealed similar dynamics with peak frequencies at 14 d following vaccination (Fig. 4C, 4D). The

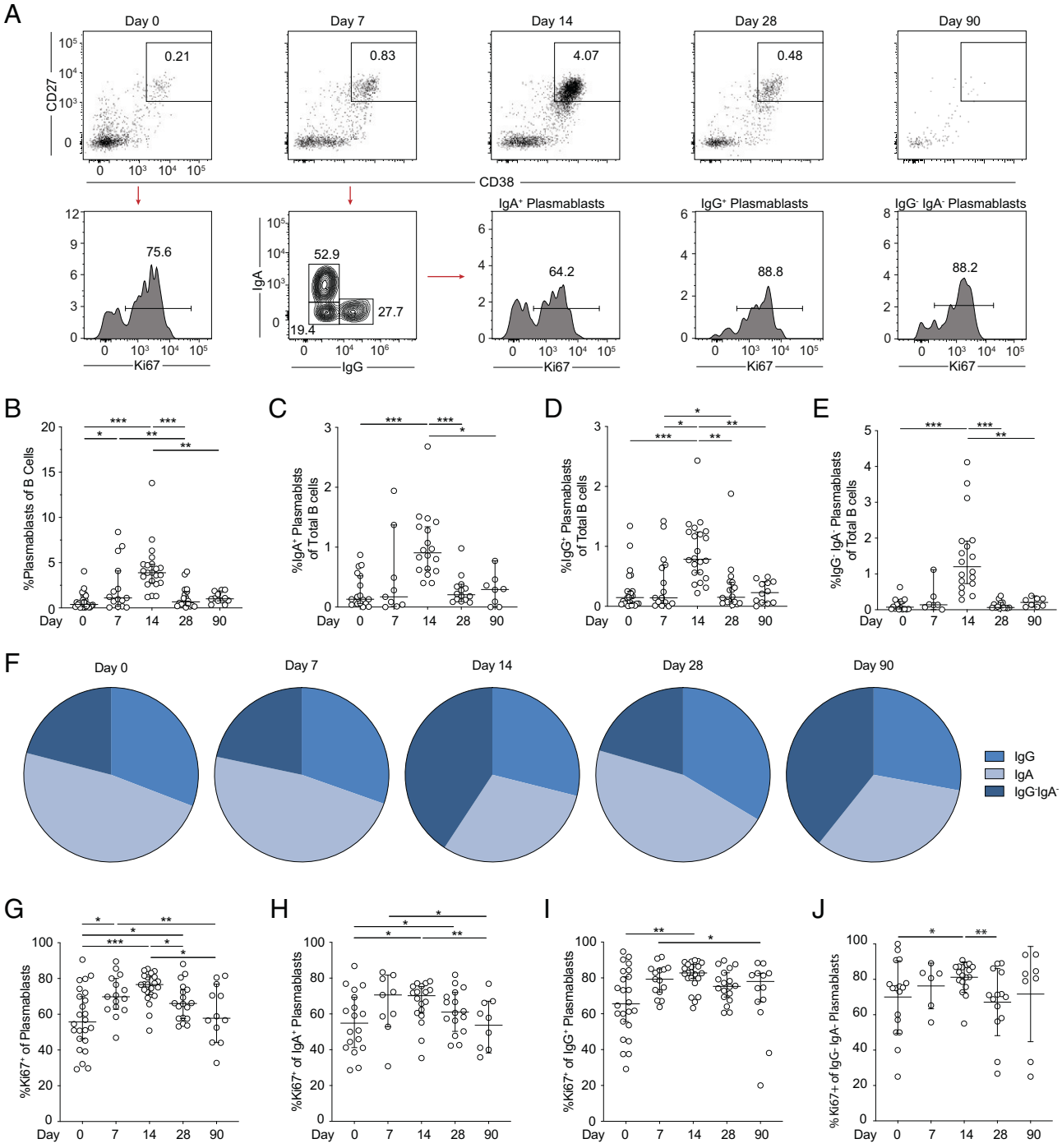

FIGURE 4. Plasmablast responses following YFV 17D vaccination. (**A**) $CD38^{high}$ and $CD27^{high}$ coexpression on $CD19^+CD20^{-/low}$ B cells define plasmablasts in freshly isolated PBMCs over time. Displayed is one representative study subject along with IgA, IgG, and Ki67 expression on each subset. (**B**) Total plasmablast and plasmablast (**C**) IgA^+, (**D**) IgG^+, and (**E**) IgA^-IgG^- subset frequencies. Median with 95% confidence interval (CI) are plotted at days 0, 7, 14, 28, and 90 following vaccination. (**F**) Proportions of Ig expression shift on plasmablasts over time. (**G**) Ki67 expression in total plasmablasts and (**H**) IgA^+, (**I**) IgG^+, and (**J**) IgA^-IgG^- and subsets plotted as median with 95% CI over time. For all plasmablast graphs, excluding IgA^+, IgA^+ $Ki67^+$, IgA^-IgG^-, and IgA^-IgG^- $Ki67^+$ subsets, day 0, $n = 24$; day 7, $n = 15$; day 14, $n = 22$; day 28, $n = 18$; and day 90, $n = 12$. For IgA^+ and $Ki67^+$ IgA^+ plasmablasts, day 0, $n = 11$; day 7, $n = 15$; day 14, $n = 20$; day 28, $n = 16$; and day 90, $n = 10$. Statistical analysis was performed using nonparametric Wilcoxon matched-pairs signed-rank test. $^*p < 0.05$, $^{**}p < 0.01$, $^{***}p < 0.001$.

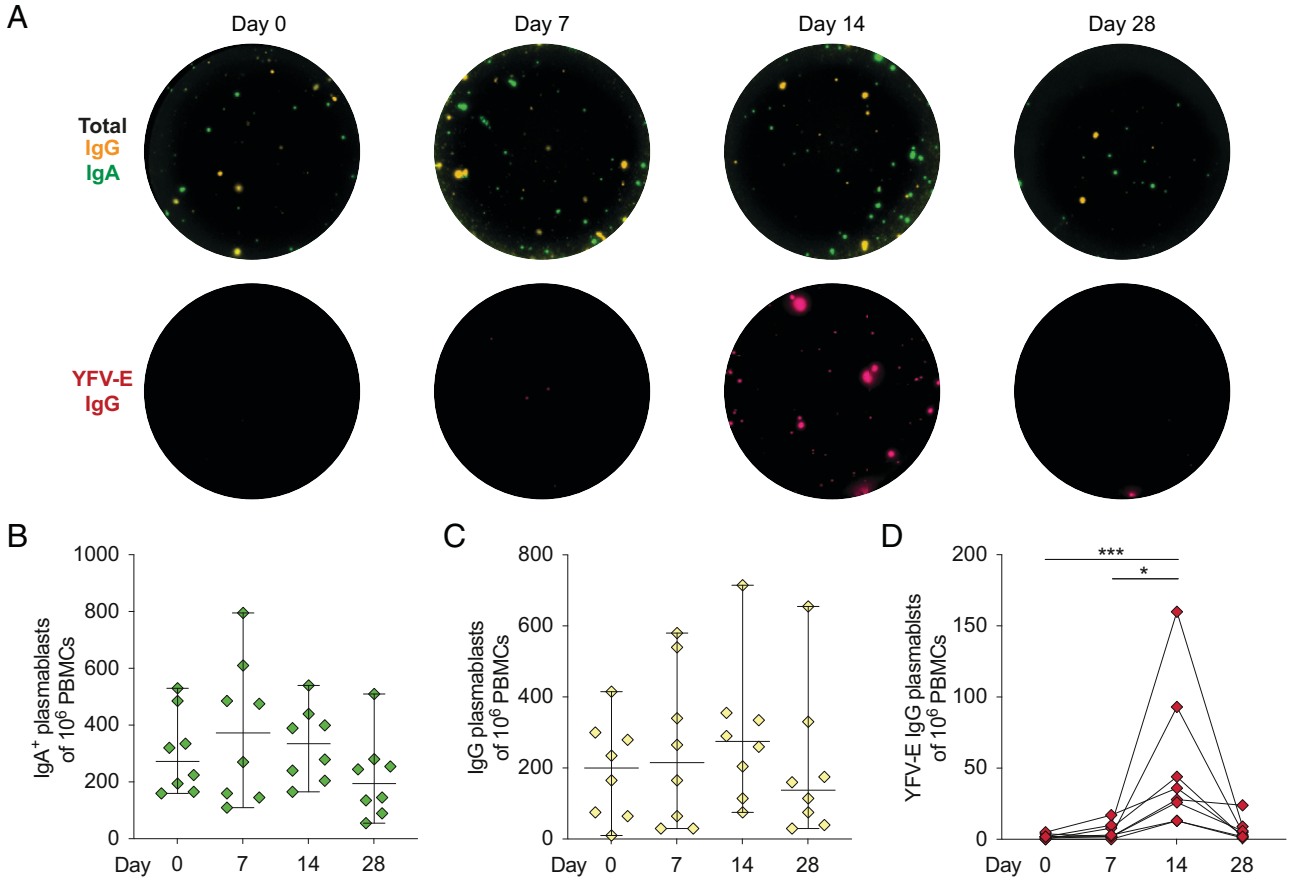

FIGURE 5. Specificity of plasmablasts following YFV 17D vaccination. (**A**) Total IgG^+ plasmablasts (yellow), IgA^+ plasmablasts (green), and YFV-E–specific IgG^+ plasmablasts (red). Shown are FluoroSpot wells from a representative study subject's cryopreserved PBMCs over time following vaccination with YFV 17D. (**B**) Total number of IgA^+ and (**C**) IgG^+ Ab-secreting cells over time following vaccination with YFV 17D. (**D**) Kinetics of YFV-E–specific IgG^+ plasmablasts per million PBMCs at days 0, 7, 14, and 28. (B and C) Median is plotted with 95% confidence interval (CI) ($n = 8$). Statistical analysis was performed using nonparametric Friedman test and corrected for multiple comparisons with Dunn multiple comparison test. $*p < 0.05$, $***p < 0.001$.

steady-state IgA^+ subset dominated the plasmablast population before and 7 d following vaccination that then shifted toward the IgG^-IgA^- subset at day 14 (Fig. 4F). The frequency of proliferating ($Ki67^+$) plasmablasts began to increase at day 7, peaked at day 14, were sustained through day 28, and then returned to baseline levels by 90 d following vaccination (Fig. 4G). Comparable kinetics of Ki67 expression were also observed in IgA^+, IgG^+, and IgA^-IgG^- plasmablast subsets (Fig. 4H, 4I). In conclusion, plasmablast responses to vaccination with YFV 17D peaked 14 d following vaccination that is 1 wk later than peak viral replication and other early cellular activation responses.

Plasmablast specificity to YFV-E protein following YFV 17D vaccination

To assess the specificity of the plasmablast responses, we developed a YFV-E–specific FluoroSpot assay using cryopreserved PBMCs from days 0, 7, 14, and 28 following YFV 17D vaccination. The assay simultaneously allowed detection of total IgG^+ and IgA^+ plasmablasts, as well as YFV-E–specific IgG^+ plasmablasts (Fig. 5A). Total IgA^+ plasmablast numbers detected by FluoroSpot revealed no significant changes over time, but a slight increase at day 7 was observed (Fig. 5B). Similarly, total IgG^+ plasmablast numbers detected by FluoroSpot did not significantly change over time but did show a trend toward increasing in numbers at day 14 (Fig. 5C). YFV-E–specific IgG^+ plasmablasts were first detectable at day 7 and peaked at day 14 before returning to low or undetectable levels at 28 d similar to IgG plasmablast kinetics assessed with flow cytometry (Fig. 5D). YFV-E–specific IgG^+ plasmablasts were found to constitute 4–83% (median 13%) of the total IgG^+ plasmablast population at their peak 14 d following vaccination (data not shown). Following assessment of kinetic and specific YFV-E plasmablast responses, we set out to investigate the generation of protective neutralizing Abs and formation of B cell memory.

Development of neutralizing Abs and correlation with plasmablast frequencies

Neutralization capacity of Abs against YFV 17D was measured in serum from 21 of the 24 study subjects. Neutralizing titers ≥5 were considered protective, as has been established by the Public Health Agency of Sweden. Neutralizing capacity was not found before vaccination except from three study subjects who were borderline positive (Fig. 6A). All study subjects tested had developed protective levels of neutralizing Abs by either day 28 or 90 following vaccination. These results demonstrate that all tested study subjects developed protective immunity against YFV. The proportion of IgG^+ plasmablast frequencies at day 14 showed a significant, positive correlation with day 90 neutralizing titers ($p = 0.0211$, $R = 0.7286$) (Fig. 6B). The IgG^+ plasmablast subset may therefore be associated with development of neutralizing Abs, suggesting they may constitute an early prognostic marker of protection.

Memory B cell frequencies in circulation following YFV 17D vaccination

Apart from induction of early plasmablast response, proportions of other B cell subsets including unswitched and switched memory B cells, naive B cells, and $CD27^-IgD^-$ double-negative B cells were

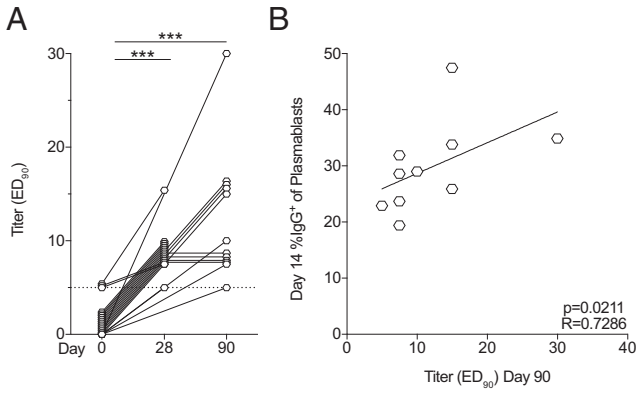

FIGURE 6. Neutralizing Ab titers correlation with IgG^+ plasmablast frequencies following YFV 17D vaccination. (**A**) Kinetics of development of neutralizing Ab titers over time (day 0, $n = 21$; day 28, $n = 17$; and day 90, $n = 12$). (**B**) Correlation between ED_{90} titers at day 90 and day 14 frequencies of IgG^+ plasmablasts ($n = 10$). Statistical analysis was performed using nonparametric Wilcoxon matched-pairs signed-rank test and nonparametric Spearman correlation test. ***$p < 0.001$.

analyzed after vaccination with YFV 17D. Memory B cells were defined as $CD27^+IgD^-CD19^+CD20^+$ cells and further divided into IgG^+ or IgA^+ subpopulations (Fig. 7A). Following YFV 17D vaccination, the total memory B cell frequencies in circulation shifted with a decrease at day 7 that remained decreased through day 14 and returned to baseline levels at day 28 (Fig. 7B). Both IgG^+ and IgA^+ memory B cells in circulation decreased following vaccination as well before returning to baseline levels at day 28 (Fig. 7C, 7D). Unswitched memory B cell, defined as $CD27^+IgD^+$ B cells, proportions also decreased in circulation at day 7 after vaccination and remained at reduced frequencies through day 14 before returning to baseline levels at day 28 (Fig. 7E). Naive B cells were defined as $CD27^-IgD^+$ B cells and were found to increase significantly in circulation at days 7 and 14 and returned to baseline levels at day 28 (Fig. 7F). Double-negative B cells were defined as $CD27^-IgD^-$ B cells. No significant changes were observed in this population over time. (Fig. 7G).

To assess the generation of vaccine-specific memory B cells, we used the same YFV-E–specific FluoroSpot assay but used polyclonal stimulated cryopreserved PBMCs from days 0, 28, and 90 following YFV 17D vaccination (Fig. 7H). A significant increase in YFV-E–specific memory B cells was observed from day 0 to both days 28 and 90 following YFV 17D vaccination (Fig. 7I). The magnitude of YFV-E–specific memory B cells revealed no significant association with earlier plasmablast levels or neutralizing Ab titers (correlations not shown). In summary, YFV-E–specific memory B cells are generated following vaccination with YFV 17D. Based on the observed changes in total and IgG^+ memory B cell frequencies in circulation 1 mo following vaccination, we went on to investigate the chemokine receptor expression patterns of memory B cells as surrogate markers of homing capacity.

Homing capacity of memory B cells following YFV 17D vaccination

The homing correlates of memory B cells, including IgG^+ memory B cells, were analyzed by assessment of expression of CCR7, CXCR3, and CXCR5 (Fig. 8A). A temporary decrease in memory B cells expressing CCR7 was observed at day 7 following vaccination (Fig. 8B). Memory B cells expressing CXCR3 decreased at day 7, followed by a gradual return at days 14 and 28 (Fig. 8C). Nearly all memory B cells in circulation at baseline were $CXCR5^+$. A significant decrease in $CXCR5^+$ memory B cells frequencies was observed at day 7 before returning to baseline levels at day 14 (Fig. 8D). Similar observations were seen with respect to homing status of the IgG^+ memory B cell subset. However, CCR7 expression changes were not significant. This also applied to the decrease in CXCR3 expression between day 0 and 7 following vaccination (Fig. 7E–G). In conclusion, following vaccination with YFV 17D, frequencies of memory B cells and IgG^+ memory B cells positive for CXCR3, CXCR5, and CCR7 were found to decrease in circulation

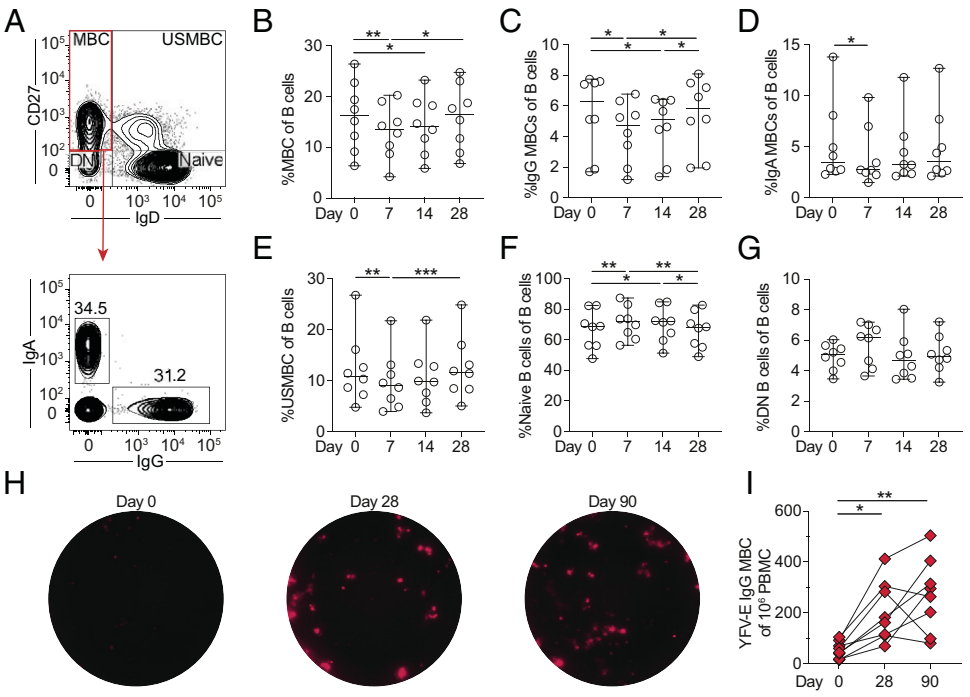

FIGURE 7. Kinetics and specificity of memory B cells following YFV 17D vaccination. (**A**) The B cell compartment was divided into $CD27^+IgD^-$ memory B cells, $CD27^+IgD^+$ unswitched memory B cells, $CD27^-IgD^-$ naive B cells, and $CD27^-IgD^-$ double-negative B cells over time. Memory B cells were further defined by their class-switched IgA or IgG expression. (**B**) Total memory B cells, (**C**) IgG^+ memory B cell, and (**D**) IgA^+ memory B cell frequencies following vaccination with YFV 17D. (**E**) Total unswitched memory B cell, (**F**) naive B cell, and (**G**) double-negative B cell frequencies over time. (**H**) Representative FluoroSpot wells at days 0, 28, and 90 detecting YFV-E^+ IgG^+ memory B cells. (**I**) The number of detectable YFV-E^+ IgG^+ memory B cells before and after vaccination at days 28 and 90 ($n = 8$). All data plotted as median with 95% confidence interval (CI) at days 0, 7, 14, and 28 after vaccination ($n = 8$). Statistical analysis was performed using nonparametric Friedman test and corrected for multiple comparisons with Dunn multiple comparison test. *$p < 0.05$, **$p < 0.01$, ***$p < 0.001$.

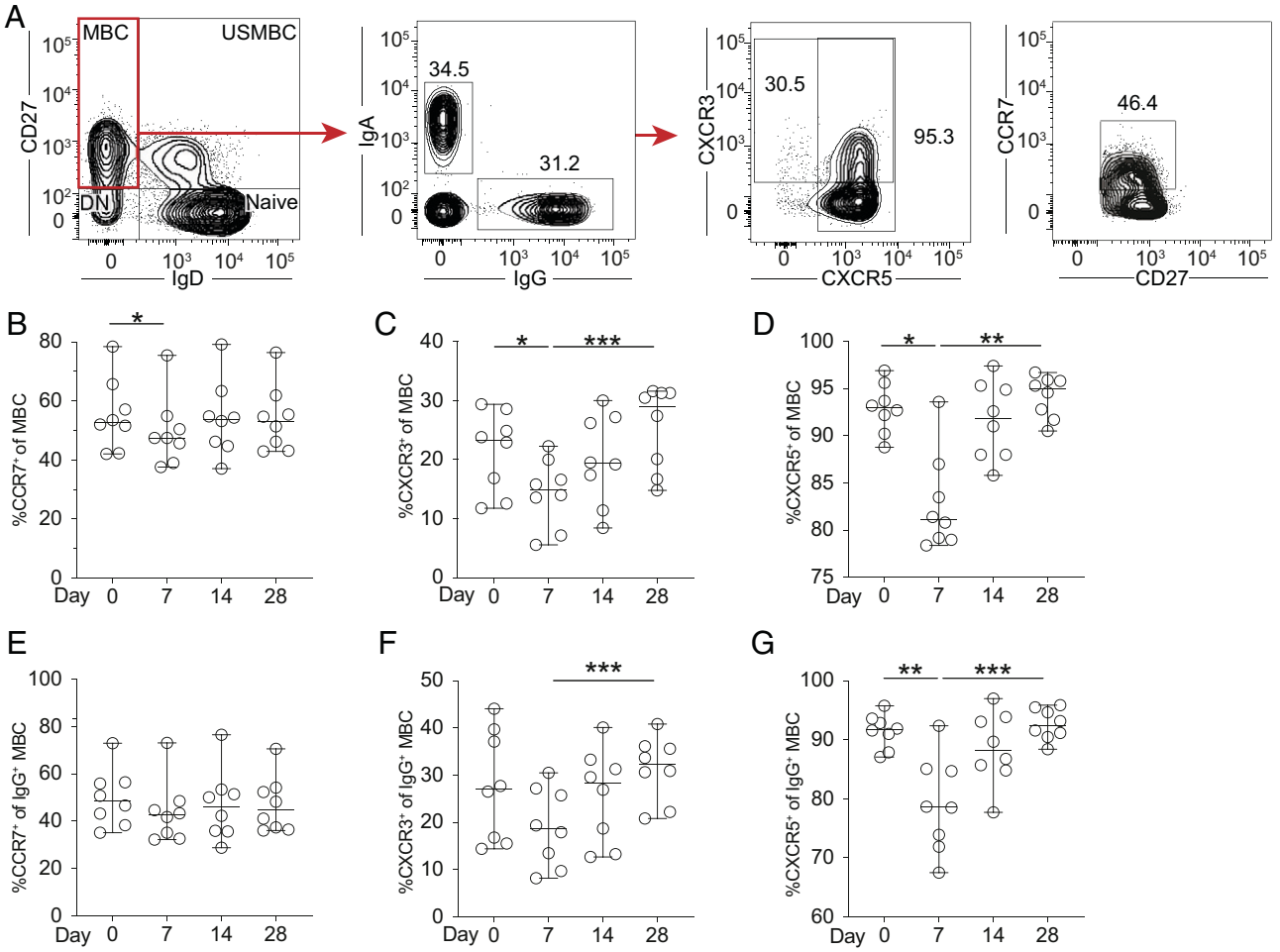

FIGURE 8. Homing characteristics of memory B cells following YFV 17D vaccination. (**A**) Gating strategy of homing receptor expression on memory B cells and IgG$^+$ subsets from a representative study subject. Frequency of CCR7, CXCR3, and CXCR5 expression on memory B cells (**B**–**D**) and IgG$^+$ memory B cells (**E**–**G**) at days 0, 7, 14, and 28 after vaccination with YFV 17D ($n = 8$). In all graphs, the median is plotted with 95% confidence interval (CI). Statistical analysis was performed using nonparametric Wilcoxon matched-pairs signed-rank test. *$p < 0.05$, **$p < 0.01$, ***$p < 0.001$.

at day 7 before returning to baseline levels in the following weeks, suggesting possible homing into secondary lymphoid organs.

Discussion

The YFV 17D vaccine has unique properties in that a single dose of the vaccine can generate lifelong immunity in humans. Numerous studies have investigated the generation of immunity toward this vaccine. Yet, more detailed insights, in particular, into the generation of specific B cell responses to the vaccine are still warranted. In this respect, in this study, we characterized the magnitude, kinetics, and specificity of B cell responses following vaccination with YFV 17D. We first assessed the events leading up to B cell response by evaluating geminal center activity through cTfh cell activation and serum CXCL13 levels, both of which increased following vaccination. Focus was then directed toward studying the magnitude and kinetics of plasmablast responses following vaccination. We observed a significant expansion of YFV-E protein specific plasmablasts at 2 wk following vaccination. Notably, plasmablast expansion was found to positively correlate with the development of neutralizing Abs.

Innate immune signatures such as the activation of both CD56^{bright} and CD56^{dim} NK cells as well as the increase of a number of soluble proinflammatory and innate markers were observed in the majority of study subjects. This innate immune activation likely suggests that these cells could contribute to and/or affect in vivo immune responses toward YFV 17D. The antiviral and proinflammatory responses observed in the current cohort are in line with type I IFN responses observed in previous reports on human vaccination with YFV 17D (19, 23). Activated NK cells can play a role in host innate immune responses by directly killing virus-infected cells as well as indirectly by secreting antiviral and proinflammatory cytokines that in turn can upregulate effector functions of other immune cells (23). Successful vaccination must not only induce early innate immune mechanisms, however, but also adaptive responses to generate immune memory.

A key feature of adaptive immune responses to infection and vaccination is the activation of germinal center reactions. Monitoring the activity of germinal centers, a major driver of high-quality Abs by somatic hypermutation (26), are of great interest to determine the mechanisms behind generation of neutralizing Abs and memory B cells following vaccination. Evaluating the magnitude of germinal center activity in secondary lymphoid tissues, however, is difficult in human studies. Recently, assessment of CXCL13 levels in serum has been shown to serve as a surrogate marker of germinal center activity (25). In the current study, CXCL13 levels were shown to increase 1 wk following YFV 17D vaccination and was shown to be sustained through 2 wk, in line with previous studies (25). Similar to CXCL13, cTfh cells have been shown to play a role in guiding Ab responses and have more recently also been used as a biomarker correlating with specific Ab generation (15, 25). A significant increase in activated

$CXCR3^+$ Th1-polarized cTfh cells was observed 14 d following YFV 17D vaccination in the current study, consistent with recent findings (16, 27). This increase in activated Th1-polarized cells was not unexpected, as these cells are the primary $CD4^+$ T cell subset involved in antiviral responses (28). They have been previously observed to expand following influenza vaccination as well as following HIV and hepatitis C virus infection (15, 29–32).

The kinetics of plasmablast responses to YFV 17D vaccination were found to be relatively consistent between individuals. Although many vaccines have been reported to induce peak plasmablast responses 7 d following vaccination in humans, plasmablast frequencies following YFV 17D vaccination peaked at day 14, as also reported by others (17, 18). This difference in kinetics, as compared with many other vaccines, may relate to the kinetics of active virus shedding (33). In line with the reasoning above, YFV 17D reaches peak viral titers roughly 7 d following vaccination, possibly explaining the concomitant specific plasmablast response 7 d later. In the current cohort, we observed a significant positive association between IgG^+ plasmablast frequencies at day 14 and neutralizing Ab titers at day 90. This suggests that plasmablasts could function as an early surrogate marker in YFV 17D vaccine studies for predicting successful protective immune responses; however, a larger cohort would be needed to determine this correlation. Additionally, a recent study found that YFV-specific mAbs, cloned from plasmablasts of vaccinated individuals, possessed higher binding avidities and neutralizing capacity than those of memory B cells 2 wk following YFV 17D vaccination. This suggests that higher-affinity B cells being selected in germinal center reactions are more prone to differentiate into plasmablasts rather than memory B cells (18, 34).

Studying the specificity of B cell responses toward vaccination at the single-cell level adds an essential layer to understanding the generation of immunological memory. The B cell ELISpot assay has long been a versatile and highly sensitive method for identifying and enumerating total and Ag-specific plasmablasts or in vitro–activated memory B cells (35, 36). In recent years, the assay has been adapted using multiple fluorophore-conjugated detection reagents to detect multiple Ags and parameters within the same well, referred to as FluoroSpot (37). We further optimized this assay to detect both total and YFV-E–specific plasmablasts. Using this method, the kinetics of YFV-E–specific plasmablasts were mapped, peaking at day 14, therefore following similar kinetics of plasmablast responses as detected by flow cytometry. The magnitude of the YFV-E–specific plasmablast response varied between study subjects. We observed that the YFV-E–specific subset constituted 4–83% of total plasmablast numbers at day 14. This wide range could be due to that the plasmablast responses being directed against other YFV Ags not tested for in the current FluoroSpot assay. Additionally, using the same FluoroSpot assay, we were able to see an increase in YFV-E–specific IgG^+ memory B cell numbers following vaccination contributing to immune memory. Five of the tested donors showed increases in specific memory B cell numbers between day 28 and 90 after YFV 17D vaccination, in align with previous work (18), but the other three study subjects' numbers decreased during the same time span. The lack of significant difference between these time points may suggest that by the first month after vaccination with YFV 17D, stable numbers of specific memory B cells may have been reached. More time points between the span or even later time points may give more insight into these levels.

In summary, we, in this study, characterized the magnitude, kinetics, and specificity of B cell responses induced by the highly effective YFV 17D vaccine, with a particular emphasis on cTfh cell, plasmablast, and memory B cell responses. An increased Th1-polarized cTfh cell activation and CXCL13 serum levels indicated germinal center activity driving the generation of neutralizing Ab titers and memory B cells in all study subjects tested. Plasmablast frequencies were found to directly correlate with the development of neutralizing Abs. The present study adds to our understanding into the generation of immunity to the live-attenuated YFV 17D vaccine.

Acknowledgments

We thank all healthy study subjects that took part in the study and research nurses B. Ekström and E. Karlsson, who sampled study subjects at the Karolinska University Hospital and Mälardalens Hospital. We also thank the members of the K. Loré and A. Smed-Sörensen groups, specifically A. Lin and S. Vangeti, who helped with logistics with respect to clinical samples. Additional thanks to C. Smedman at Mabtech for feedback on the FluoroSpot optimization protocol.

Disclosures

The authors have no financial conflicts of interest.

References

1. Giovanetti, M., M. C. L. de Mendonça, V. Fonseca, M. A. Mares-Guia, A. Fabri, J. Xavier, J. G. de Jesus, T. Gräf, C. D. Dos Santos Rodrigues, C. C. Dos Santos, et al. 2019. Yellow fever virus reemergence and spread in Southeast Brazil, 2016-2019. [Published erratum appears in 2020 *J. Virol.* 94: e02008-19.] *J. Virol.* 94: e01623-19.
2. Staples, J. E., J. A. Bocchini, Jr., L. Rubin, and M. Fischer; Centers for Disease Control and Prevention (CDC). 2015. Yellow fever vaccine booster doses: Recommendations of the advisory committee on immunization practices, 2015. *MMWR Morb. Mortal. Wkly. Rep.* 64: 647–650.
3. Monath, T. P., M. Gershman, J. Erin Staples, and A. D. T. Barrett. 2012. Yellow fever vaccine. In *Vaccines*, 6th Ed. S. Plotkin, W. Orenstein, and P. Offit, eds. Elsevier, Philadelphia, PA, p. 870–968.
4. Blom, K., M. Braun, M. A. Ivarsson, V. D. Gonzalez, K. Falconer, M. Moll, H.-G. Ljunggren, J. Michaëlsson, and J. K. Sandberg. 2013. Temporal dynamics of the primary human T cell response to yellow fever virus 17D as it matures from an effector- to a memory-type response. *J. Immunol.* 190: 2150–2158.
5. Akondy, R. S., N. D. Monson, J. D. Miller, S. Edupuganti, D. Teuwen, H. Wu, F. Quyyumi, S. Garg, J. D. Altman, C. Del Rio, et al. 2009. The yellow fever virus vaccine induces a broad and polyfunctional human memory CD8+ T cell response. *J. Immunol.* 183: 7919–7930.
6. James, E. A., R. E. LaFond, T. J. Gates, D. T. Mai, U. Malhotra, and W. W. Kwok. 2013. Yellow fever vaccination elicits broad functional CD4+ T cell responses that recognize structural and nonstructural proteins. *J. Virol.* 87: 12794–12804.
7. Watson, A. M., and W. B. Klimstra. 2017. T cell-mediated immunity towards yellow fever virus and useful animal models. *Viruses* 9: 77.
8. Gotuzzo, E., S. Yactayo, and E. Córdova. 2013. Efficacy and duration of immunity after yellow fever vaccination: systematic review on the need for a booster every 10 years. *Am. J. Trop. Med. Hyg.* 89: 434–444.
9. Wieten, R. W., E. F. F. Jonker, E. M. M. van Leeuwen, E. B. M. Remmerswaal, I. J. M. Ten Berge, A. W. de Visser, P. J. J. van Genderen, A. Goorhuis, L. G. Visser, M. P. Grobusch, and G. J. de Bree. 2016. A single 17D yellow fever vaccination provides lifelong immunity; characterization of yellow-fever-specific neutralizing antibody and T-cell responses after vaccination. *PLoS One* 11: e0149871.
10. Lu, X., H. Xiao, S. Li, X. Pang, J. Song, S. Liu, H. Cheng, Y. Li, X. Wang, C. Huang, et al. 2019. Double lock of a human neutralizing and protective monoclonal antibody targeting the yellow fever virus envelope. *Cell Rep.* 26: 438–446.e5.
11. Daffis, S., R. E. Kontermann, J. Korimbocus, H. Zeller, H. D. Klenk, and J. Ter Meulen. 2005. Antibody responses against wild-type yellow fever virus and the 17D vaccine strain: characterization with human monoclonal antibody fragments and neutralization escape variants. *Virology* 337: 262–272.
12. Victora, G. D., and M. C. Nussenzweig. 2012. Germinal centers. *Annu. Rev. Immunol.* 30: 429–457.
13. Stebegg, M., S. D. Kumar, A. Silva-Cayetano, V. R. Fonseca, M. A. Linterman, and L. Graca. 2018. Regulation of the germinal center response. *Front. Immunol.* 9: 2469.
14. Morita, R., N. Schmitt, S. E. Bentebibel, R. Ranganathan, L. Bourdery, G. Zurawski, E. Foucat, M. Dullaers, S. Oh, N. Sabzghabaei, et al. 2011. Human blood CXCR5(+)CD4(+) T cells are counterparts of T follicular cells and contain specific subsets that differentially support antibody secretion. *Immunity* 34: 108–121.
15. Lindgren, G., S. Ols, F. Liang, E. A. Thompson, A. Lin, F. Hellgren, K. Bahl, S. John, O. Yuzhakov, K. J. Hassett, et al. 2017. Induction of robust B cell responses after influenza mRNA vaccination is accompanied by circulating hemagglutinin-specific ICOS+ PD-1+ CXCR3+ T follicular helper cells. [Published erratum appears in 2019 *Front Immunol.* 10: 614.] *Front. Immunol.* 8: 1539.
16. Huber, J. E., J. Ahlfeld, M. K. Scheck, M. Zaucha, K. Witter, L. Lehmann, H. Karimzadeh, M. Pritsch, M. Hoelscher, F. von Sonnenburg, et al. 2020. Dynamic changes in circulating T follicular helper cell composition predict neutralising

antibody responses after yellow fever vaccination. *Clin. Transl. Immunology* 9: e1129.
17. Kohler, S., N. Bethke, M. Böthe, S. Sommerick, M. Frentsch, C. Romagnani, M. Niedrig, and A. Thiel. 2012. The early cellular signatures of protective immunity induced by live viral vaccination. *Eur. J. Immunol.* 42: 2363–2373.
18. Wec, A. Z., D. Haslwanter, Y. N. Abdiche, L. Shehata, N. Pedreño-Lopez, C. L. Moyer, Z. A. Bornholdt, A. Lilov, J. H. Nett, R. K. Jangra, et al. 2020. Longitudinal dynamics of the human B cell response to the yellow fever 17D vaccine. *Proc. Natl. Acad. Sci. USA* 117: 6675–6685.
19. Querec, T. D., R. S. Akondy, E. K. Lee, W. Cao, H. I. Nakaya, D. Teuwen, A. Pirani, K. Gernert, J. Deng, B. Marzolf, et al. 2009. Systems biology approach predicts immunogenicity of the yellow fever vaccine in humans. *Nat. Immunol.* 10: 116–125.
20. Miller, J. D., R. G. van der Most, R. S. Akondy, J. T. Glidewell, S. Albott, D. Masopust, K. Murali-Krishna, P. L. Mahar, S. Edupuganti, S. Lalor, et al. 2008. Human effector and memory CD8+ T cell responses to smallpox and yellow fever vaccines. *Immunity* 28: 710–722.
21. Assarsson, E., M. Lundberg, G. Holmquist, J. Björkesten, S. B. Thorsen, D. Ekman, A. Eriksson, E. Rennel Dickens, S. Ohlsson, G. Edfeldt, et al. 2014. Homogenous 96-plex PEA immunoassay exhibiting high sensitivity, specificity, and excellent scalability. *PLoS One* 9: e95192.
22. Vene, S., M. Haglund, O. Vapalahti, and A. Lundkvist. 1998. A rapid fluorescent focus inhibition test for detection of neutralizing antibodies to tick-borne encephalitis virus. *J. Virol. Methods* 73: 71–75.
23. Marquardt, N., M. A. Ivarsson, K. Blom, V. D. Gonzalez, M. Braun, K. Falconer, R. Gustafsson, A. Fogdell-Hahn, J. K. Sandberg, and J. Michaëlsson. 2015. The human NK cell response to yellow fever virus 17d is primarily governed by NK cell differentiation independently of NK cell education. *J. Immunol.* 195: 3262–3272.
24. Monaco, G., B. Lee, W. Xu, S. Mustafah, Y. Y. Hwang, C. Carré, N. Burdin, L. Visan, M. Ceccarelli, M. Poidinger, et al. 2019. RNA-Seq signatures normalized by mRNA abundance allow absolute deconvolution of human immune cell types. *Cell Rep.* 26: 1627–1640.e7.
25. Havenar-Daughton, C., M. Lindqvist, A. Heit, J. E. Wu, S. M. Reiss, K. Kendric, S. Bélanger, S. P. Kasturi, E. Landais, R. S. Akondy, et al; IAVI Protocol C Principal Investigators. 2016. CXCL13 is a plasma biomarker of germinal center activity. *Proc. Natl. Acad. Sci. USA* 113: 2702–2707.
26. Mesin, L., J. Ersching, and G. D. Victora. 2016. Germinal center B cell dynamics. *Immunity* 45: 471–482.
27. DeGottardi, Q., T. J. Gates, J. Yang, E. A. James, U. Malhotra, I. T. Chow, Y. Simoni, M. Fehlings, E. W. Newell, H. A. DeBerg, and W. W. Kwok. 2020. Ontogeny of different subsets of yellow fever virus-specific circulatory $CXCR5^+$ $CD4^+$ T cells after yellow fever vaccination. *Sci. Rep.* 10: 15686.
28. Snell, L. M., I. Osokine, D. H. Yamada, J. R. De la Fuente, H. J. Elsaesser, and D. G. Brooks. 2016. Overcoming CD4 Th1 cell fate restrictions to sustain antiviral CD8 T cells and control persistent virus infection. *Cell Rep.* 16: 3286–3296.
29. Bentebibel, S. E., S. Khurana, N. Schmitt, P. Kurup, C. Mueller, G. Obermoser, A. K. Palucka, R. A. Albrecht, A. Garcia-Sastre, H. Golding, and H. Ueno. 2016. ICOS(+)PD-1(+)CXCR3(+) T follicular helper cells contribute to the generation of high-avidity antibodies following influenza vaccination. *Sci. Rep.* 6: 26494.
30. Locci, M., C. Havenar-Daughton, E. Landais, J. Wu, M. A. Kroenke, C. L. Arlehamn, L. F. Su, R. Cubas, M. M. Davis, A. Sette, et al; International AIDS Vaccine Initiative Protocol C Principal Investigators. 2013. Human circulating PD-1+CXCR3-CXCR5+ memory Tfh cells are highly functional and correlate with broadly neutralizing HIV antibody responses. *Immunity* 39: 758–769.
31. Maloy, K. J., C. Burkhart, T. M. Junt, B. Odermatt, A. Oxenius, L. Piali, R. M. Zinkernagel, and H. Hengartner. 2000. CD4(+) T cell subsets during virus infection. Protective capacity depends on effector cytokine secretion and on migratory capability. *J. Exp. Med.* 191: 2159–2170.
32. Zhang, J., W. Liu, B. Wen, T. Xie, P. Tang, Y. Hu, L. Huang, K. Jin, P. Zhang, Z. Liu, et al. 2019. Circulating $CXCR3^+$ Tfh cells positively correlate with neutralizing antibody responses in HCV-infected patients. *Sci. Rep.* 9: 10090.
33. Lee, F. E., A. R. Falsey, J. L. Halliley, I. Sanz, and E. E. Walsh. 2010. Circulating antibody-secreting cells during acute respiratory syncytial virus infection in adults. *J. Infect. Dis.* 202: 1659–1666.
34. Paus, D., T. G. Phan, T. D. Chan, S. Gardam, A. Basten, and R. Brink. 2006. Antigen recognition strength regulates the choice between extrafollicular plasma cell and germinal center B cell differentiation. *J. Exp. Med.* 203: 1081–1091.
35. Giannini, S. L., E. Hanon, P. Moris, M. Van Mechelen, S. Morel, F. Dessy, M. A. Fourneau, B. Colau, J. Suzich, G. Losonksy, et al. 2006. Enhanced humoral and memory B cellular immunity using HPV16/18 L1 VLP vaccine formulated with the MPL/aluminium salt combination (AS04) compared to aluminium salt only. *Vaccine* 24: 5937–5949.
36. Czerkinsky, C. C., L. Å. Nilsson, H. Nygren, O. Ouchterlony, and A. Tarkowski. 1983. A solid-phase enzyme-linked immunospot (ELISPOT) assay for enumeration of specific antibody-secreting cells. *J. Immunol. Methods* 65: 109–121.
37. Gazagne, A., E. Claret, J. Wijdenes, H. Yssel, F. Bousquet, E. Levy, P. Vielh, F. Scotte, T. L. Goupil, W. H. Fridman, and E. Tartour. 2003. A Fluorospot assay to detect single T lymphocytes simultaneously producing multiple cytokines. *J. Immunol. Methods* 283: 91–98.